npj climate and atmospheric science

www.nature.com/npjclimatsci

ARTICLE OPEN

Check for updates

Impacts of tropical cyclones on the global water budget

Albenis Pérez-Alarcón[1,2], Patricia Coll-Hidalgo[1], José C. Fernández-Alvarez[1,2], Ricardo M. Trigo[3,4], Raquel Nieto[1] and Luis Gimeno[1]✉

Tropical cyclones (TCs) require substantial amounts of moisture for their genesis and development, acting as important moisture drivers from the ocean to land and from tropical to subtropical and extratropical regions. Quantifying anomalous moisture transport related to TCs is crucial for understanding long-term TC-induced changes in the global hydrological cycle. Our results highlight that, in terms of the global water budget, TCs enhance moisture transport from evaporative regions and precipitation over sink regions, leading to predominantly anomalous positive surface freshwater flux areas over the tropics and more regionally concentrated negative areas over the Intertropical Convergence Zone. Furthermore, we detected seasonal variability in the impact of TC on the hydrological cycle, which is closely related to the annual and seasonal TC frequency. Our analysis also revealed a global statistically significant drop (~40 mm year^{-1}) in TC-induced surface freshwater fluxes from 1980 to 2018 in response to the increasing sea surface temperature and slightly decrease in global TC frequency and lifetime in the last two decades. These findings have important implications for predicting the impacts of TCs on the hydrological cycle under global warming conditions.

npj Climate and Atmospheric Science (2023)6:212 ; https://doi.org/10.1038/s41612-023-00546-5

INTRODUCTION

Tropical cyclones (TCs) are critical for transferring moisture from the tropics to mid-latitudes and high latitudes[1,2] and from the ocean to land[3,4], thereby influencing weather patterns in tropical and subtropical regions worldwide [e.g. ref. [5]] and playing a crucial role in the atmospheric branch of the global hydrological cycle[3,4,6,7]. While relevant in these roles, the contribution of TCs to poleward water vapour transport from tropical to extratropical regions across the mid-latitudes globally is substantially smaller than that of atmospheric rivers[8]. Nonetheless, intense convective activity during TCs induces a vast amount of water vapour that is redistributed across the atmosphere and can produce notable precipitation totals in terrestrial regions[6,7], providing moisture to areas that may experience dry conditions[9]. However, impacts of TCs are associated with substantial environmental disturbances as well as socioeconomic and human losses caused by extreme compound events, such as strong winds, heavy rainfall, storm surges, flash flooding, and landslide[10,11].

Atmospheric moisture availability is crucial for TC genesis and development[12]. Indeed, modelling and theoretical studies have demonstrated that an increase (decrease) in mid-level water vapour content enhances (inhibits) TC intensification[13,14]. Furthermore, understanding the origin of moisture for precipitation produced by TCs is key to significantly assisting in risk analysis and mitigating the often strong associated impacts. Recently, Pérez-Alarcón et al.[15–17] revealed that precipitating moisture was predominantly highest from sources close to the TC positions. Likewise, large-scale atmospheric circulation patterns in each region drove the moisture towards the TC locations.

Improving our knowledge of moisture transport is crucial for investigating extreme precipitation events[18,19]. Anomalous moisture transport caused by changes in large-scale circulation is a key factor in long-term changes in extreme precipitation[20]. Thus, TCs contribute significantly to onshore moisture transport. Because moisture and heat fluxes from the warm sea surface are the principal fuels for TCs[13], previous studies have been mainly focused on the TC water budget[21–26], the origin of moisture for TCs precipitation[15–17,27], the contribution of TCs to monthly and annual precipitation totals in tropical and subtropical latitudes[6,7] or the TC-related onshore moisture transport[3,4]. For example, moisture convergence is the main contributor to TC rainfall[24,26]; TCs are responsible for approximately 14–19% of the net onshore moisture driven towards North America[3] and their precipitation represents a significant fraction of the annual precipitation totals at regional, continental and even global scales[4,6]. Additionally, part of the moisture gained by TCs from the ocean evaporation is brought about by the storm itself[22], so TCs can induce anomalous moisture fluxes towards their locations. However, few studies [e.g. refs. [28–31]] have investigated anomalies in moisture transport by TCs, which are necessary to understand the role of TCs in regional and global hydrological cycles. Extreme precipitation and moisture flux are positively correlated[3]. On this basis, the spatial pattern of anomalous moisture convergence tends to agree with the regions of anomalous cyclonic circulation in the tropical northeastern Pacific Ocean[28]. In particular, a climatological analysis of vertically integrated water vapour transport from hurricanes Matthew (2016) and Florence (2018) revealed the critical role of anomalous moisture flow from the Atlantic Ocean in producing extreme rainfall in North and South Carolina[30].

Based on these previous studies and large-scale water and energy budgets, it remains unclear what happens with atmospheric moisture before it arrives at TC locations, which areas experience more evaporation than precipitation during TCs and vice versa, and whether the long-term tendencies of these anomalous moisture fluxes are linked to global warming. Therefore, this knowledge gap and the projected increase in atmospheric water vapour content at a rate of ~6–7% per degree of sea surface warming (on the basis of the Clausius–Clapeyron equation)[32–34] warrant further examination of the anomalous

[1]Centro de Investigación Mariña, Universidade de Vigo, Environmental Physics Laboratory (EPhysLab), Campus As Lagoas s/n, 32004 Ourense, Spain. [2]Departamento de Meteorología, Instituto Superior de Tecnologías y Ciencias Aplicadas, Universidad de La Habana, 10400 La Habana, Cuba. [3]Instituto Dom Luiz (IDL), Facultade de Ciências, Universidade de Lisboa, Lisbon, Portugal. [4]Departamento de Meteorologia, Universidade Federal do Rio de Janeiro, Rio de Janeiro 21941-919, Brazil. ✉email: l.gimeno@uvigo.es

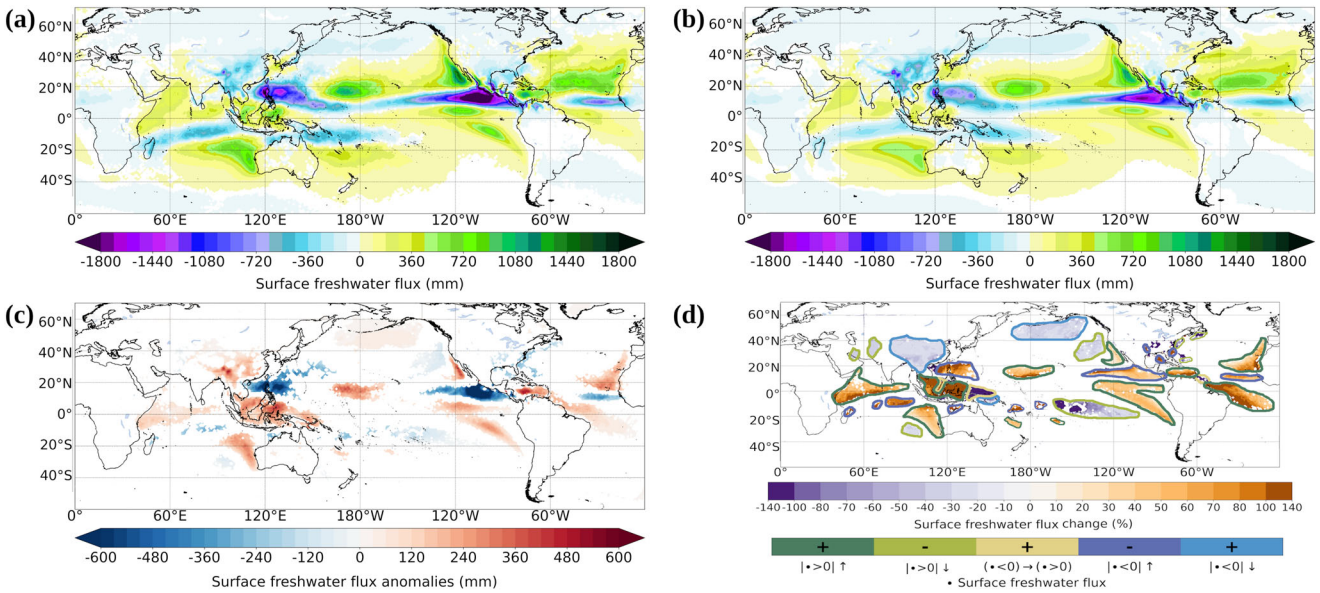

Fig. 1 Annual TC-related surface freshwater flux. a Surface freshwater flux (in mm) linked to tropical cyclones (TCs). **b** Climatological surface freshwater fluxes for the same dates of TCs. Greenish shade represents areas where the evaporation exceeds precipitation (positive surface freshwater flux) and bluish shade areas where the precipitation is higher than the evaporation (negative surface freshwater flux). **c** Significative surface freshwater flux anomalies (computing (**a**) − (**b**)) during TCs. The level of significance at 95% was calculated using the Wilcoxon signed-rank test. **d** Surface freshwater fluxes anomalies in (%) during TCs. The percentage was computed as the difference between the TC-related surface freshwater flux and the climatological value, divided by the latter. The contour lines are schematic representations of areas of positive and negative surface freshwater flux anomalies and the corresponding change during TCs, and the arrows illustrate the changes in the surface freshwater flux during TCs relative to the climatological value. Supplementary Table 1 shows a comprehensive description of all annotations shown in panel (d). The analysis was performed using the FLEXible PARTicle dispersion model (FLEXPART) outputs fed by the European Centre for Medium-Range Weather Forecast ERA-Interim reanalysis from 1980 to 2018.

moisture fluxes induced by TCs and their impacts on regional and global hydrological cycles.

The extensive application of Lagrangian moisture tracking models[35,36] to investigate moisture source-sink relationships has been adopted in the last decade for examining anomalous moisture transport[37,38] and TCs[15–17,27]. Here, we performed a global analysis to identify areas where TCs induced anomalous surface freshwater flux (TC-induced evaporation minus TC-induced precipitation) between 1980 and 2018. We focused on quantifying the anomalies in moisture fluxes induced by TCs at the regional and global scales by applying a Lagrangian tracking method using global outputs from the FLEXible PARTicle dispersion model (FLEXPART)[39]. More details on the FLEXPART simulations and moisture tracking approach are available in the 'Methods' section.

RESULTS

Anomalous surface freshwater flux

TCs require substantial moisture availability to form and intensify[12,13] and consequently produce precipitation along their trajectories[27,40–42]. On this basis, TCs should induce anomalous moisture fluxes. Therefore, we examined the anomalies in TC-induced evaporation-precipitation patterns by applying a Lagrangian moisture tracking approach[43,44] to the pathways of atmospheric parcels within the outer radius of TCs from the global outputs of the FLEXPART model[39] fed by the ERA-Interim reanalysis data from the European Centre for Medium-Range Weather Forecasts (ECMWF)[45]. For each TC position, we first computed the TC-related surface freshwater flux (*E-P*) pattern (see the 'Methods' section) and then estimated the annual surface freshwater flux and the corresponding anomalies over the study period for the same TC dates (Fig. 1).

Contrasting the spatial distribution of the annual surface freshwater flux linked to TCs (Fig. 1a) and the climatological pattern for the same TC time step during the study period (Fig. 1b), TCs generally induced more evaporation and precipitation than the climatological values in the same areas (also in agreement with the annual surface freshwater flux field, Supplementary Fig. 1). As expected, during TC days, the widespread increase in evaporation (~>50%, Fig. 1d) implies anomalous positive surface freshwater flux areas larger than negative ones over the tropics because the increased precipitation associated with TCs is more regionally concentrated (Fig. 1c). The outstanding value of the large maximum of positive freshwater flux anomalies resulted from the relevance of TCs to moisture transport. These highly evaporative regions agree with previous findings that focused on the origin of moisture for the precipitation of TCs[15–17]. Meanwhile, the pattern of sink regions for TC days coincided with climatological areas of higher precipitation than evaporation (Fig. 1a and Supplementary Fig. 1), namely the Intertropical Convergence Zone (ITCZ) in both hemispheres[46], the Western North Pacific Monsoon trough region, and southeastern Asia[47]. The nuclei of change (~50–80%, Fig. 1d) in the negative surface freshwater flux anomalies are located in the western North Pacific Ocean (WNP) and northeast Pacific Ocean (NEPAC), which are intrinsically related to the higher TC frequency in these basins, accounting for ~31%[48] and ~20%[49] of the annual global TCs, respectively. Interestingly, based on a simple inspection of Fig. 1c, d, positive surface freshwater flux anomalies over southern Asia indicate a reduction in precipitation over this region during TCs by comparing analogous dates during the study period. Overall, the spatial pattern of the TC-related surface freshwater flux (Fig. 1 and Supplemenyary Fig. 2) revealed that the impact of TCs on the hydrological cycle is more significant in the Northern Hemisphere than in the Southern Hemisphere, which is likely related to the substantially larger number of TCs formed in the Northern Hemisphere (Supplementary Figs. 3 and 4).

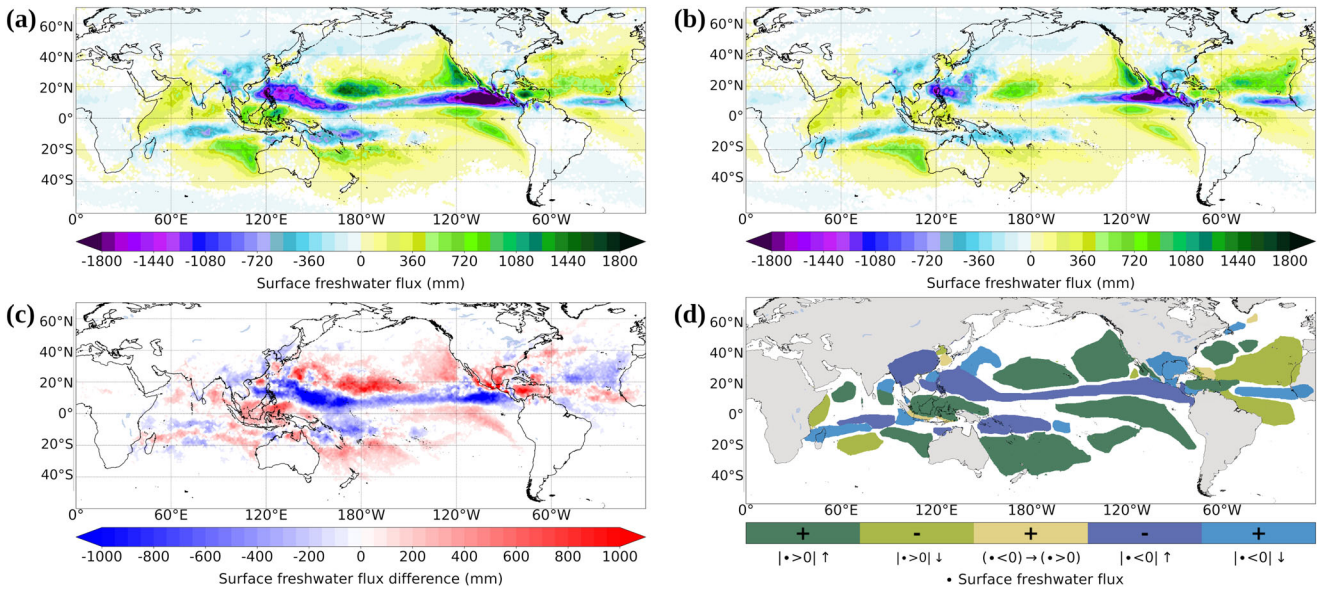

Fig. 2 Influence of ENSO on the annual TC-related surface freshwater flux. Surface freshwater flux (in mm), linked to tropical cyclones during **a** warm (El Niño) and **b** cold (La Niña) phases of ENSO. Greenish-shaded regions represent areas where evaporation exceeds precipitation (positive surface freshwater flux), whereas bluish regions indicate areas where precipitation is higher than evaporation (negative surface freshwater flux). **c** Significant differences in surface freshwater flux during El Niño and La Niña years (computing (**a**)−(**b**)). Significance was calculated at the 95% level using the Wilcoxon signed-rank test. **d** Schematic representation of areas of positive and negative surface freshwater flux differences (from (**c**)) and the corresponding change during El Niño years; arrows illustrate the changes in the surface freshwater flux during El Niño years relative to those during La Niña years. Supplementary Table 1 shows a comprehensive description of all annotations shown in (**d**). The analysis was performed using FLEXible PARTicle dispersion model (FLEXPART) outputs fed by the European Centre for Medium-Range Weather Forecast ERA-Interim reanalysis from 1980 to 2018.

Due to the impact of El Niño-Southern Oscillation (ENSO) on the basin-scale TC frequency, we also examined the possible influence of ENSO on the anomalous moisture transport induced by TCs from 1980 to 2018 (Fig. 2). The negative surface freshwater flux (precipitation>evaporation) induced by TCs was noticeably higher in absolute value during El Niño years than during La Niña years over southern Asia and along the average position of the ITCZ in the Pacific and eastern Indian Oceans, and lower over the Gulf of Mexico, southern United States and the Atlantic and western Indian Oceans ITCZ region during TC season (dark blue shaded area in Fig. 2d). Similarly, the positive surface freshwater flux during El Niño exceeded that during La Niña over large sectors of both the northern and southern Pacific Ocean, Wharton and Perth basins, Arabian Sea, southern Bay of Bengal, Caribbean Sea, and western North Atlantic (dark green areas in Fig. 2d). Meanwhile, it decreased in the Atlantic Ocean north and south of the ITCZ, central Indian Ocean south of the ITCZ, and Somali Basin in the western Indian Ocean (lime-green areas in Fig. 2d).

Surface freshwater flux trend

TCs have marked year-to-year variability at basin and global scales (Supplementary Fig. 4). Therefore, we also examined the annual trend in TC-related surface freshwater flux values from 1980 to 2018 (Fig. 3). By matching areas with statistically significant trends ($p < 0.05$) in the TC-related surface freshwater flux shown in Fig. 3 with the moisture source and sinks regions displayed in Fig. 1a, we detected an overall reduction of the TC-related surface freshwater flux across the globe, especially in the South Indian and Pacific Ocean basins. The sink regions over the eastern tropical Pacific Ocean and the Philippine Sea exhibited the highest decrease, dropping by up to 70–90 and 40–60 mm year^{-1}, respectively. Meanwhile, the surface freshwater flux over source regions has similarly decreased over the last four decades, exhibiting the highest drop over the Wharton and Perth basins in the South Indian Ocean at a rate of ~40–90 mm year^{-1}.

The sensitivity of TC-related surface freshwater flux to sea surface temperature (SST) is also investigated. The annual mean SST was computed from the Daily Optimum Interpolation Sea Surface Temperature dataset[50] within the region of higher TC activity in each basin (see 'Methods' and Supplementary Fig. 5) for the dates of TC occurrence. By matching the spatial patterns of SST trends and the Spearman correlation coefficients between SST- and TC-related surface freshwater flux with the spatial distribution of TC-related surface freshwater flux trends (Fig. 3), two features stand out: SST exhibits a basin-wide statistically significant increasing trends and inversely correlates with the TC-related surface freshwater flux. It is worth noting that positive correlation coefficients coincide with sink regions (Fig. 1a), and thereby, TC-related surface freshwater flux decreases with increasing SST. The former feature provides evidence of global warming, reaching noticeable values of 0.035–0.04 °C year^{-1} in NEPAC and South Indian Ocean (SIO) basins (Supplementary Fig. 6a), and the second reveals a closer relationship between SST and TC-related surface freshwater flux. The sign of Spearman correlation coefficients coincides with that from TC-related surface freshwater flux trends (Supplementary Fig. 6b). Overall, an increase in SST leads to a decrease in TC-related surface freshwater flux, which suggests that TC-induced precipitation is evolving to become similar to TC-induced evaporation. To examine this hypothesis, we computed the differences between the annual time series of basin and global scales lifetime accumulated evaporation and precipitation within the TC outer radius from the ERA-Interim reanalysis and Multi-Source Weighted-Ensemble Precipitation version 2 database (MSWEP V2)[51]. While the lifetime accumulated TC-induced evaporation minus precipitation within the cyclone outer radius (Supplementary Fig. 7) significantly increases in North Atlantic ocean (NATL) in agreement with Hallam et al.[52], it exhibits an overall decrease in the remaining basins and globally, being statistically significant for the South Pacific and WNP basins and at global scale. Although the lifetime accumulated precipitation (evaporation) is highly

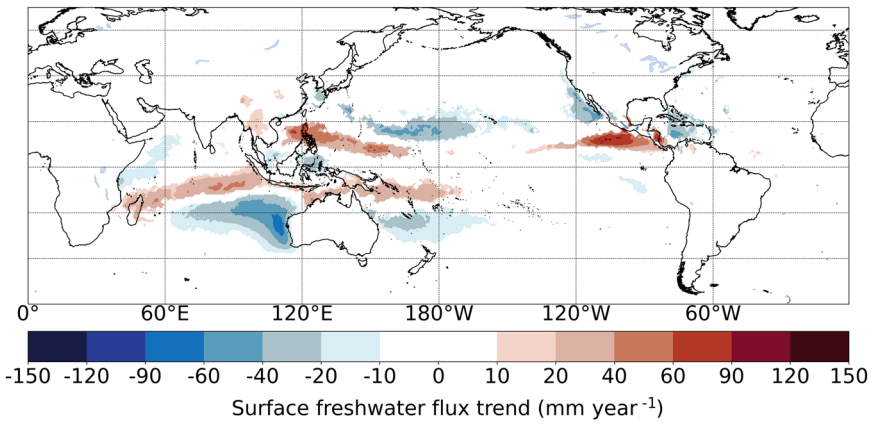

Fig. 3 Annual trend in TC-related surface freshwater flux. Filled areas show statistically significant surface freshwater flux tendencies (95% level of significance) between 1980 and 2018. A positive trend indicates a reduction in the surface freshwater flux over sink regions and negative values represent a decreasing trend in the surface freshwater flux over source regions. TCs sink and source regions are clearly identified in Fig. 1a.

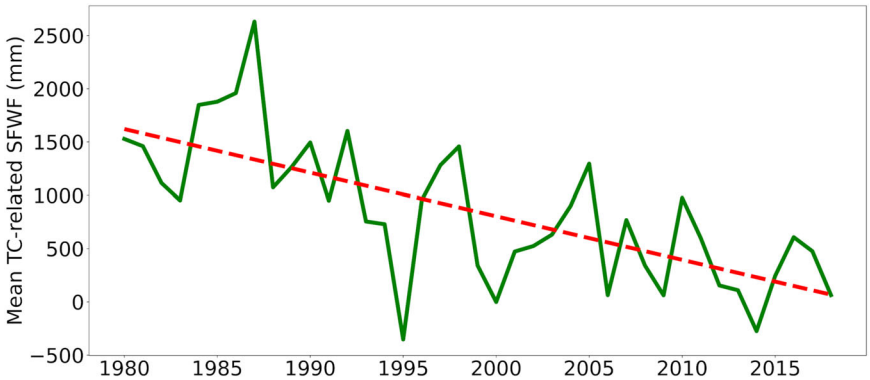

Fig. 4 Annual global TC-related surface freshwater flux. The green line denotes the annual global TC-related surface freshwater flux (SFWF) and the dashed red line shows its statistically significant (p<0.05) decreasing linear trend. The analysis was performed using FLEXible PARTicle dispersion model (FLEXPART) outputs fed by the European Centre for Medium-Range Weather Forecast ERA-Interim reanalysis from 1980 to 2018.

dependent on TC frequency (Supplementary Fig. 4) and duration (Supplementary Fig. 8), it is an important metric for the influence of TCs on global water budgets[53]. While TC lifetime significantly increases in NATL, it decreases in WNP. Globally we did not detect any statistically significant trend in TC lifetime, thus TC activity in WNP seems to have a modulating role on the influence of TCs on the global hydrological cycle. In fact, WNP achieves ~30% and ~35% of annual global TC frequency and 6-hourly track points, respectively. The global trends of the differences between lifetime accumulated TC-induced evaporation and precipitation within the outer radius highlight the marked influence of TC frequency in the TC-related freshwater flux, as discussed above.

The overall decreasing trend in the TC-related surface freshwater flux is also found by computing its annual value. During the last four decades we found decreasing trends for all basins, except the NEPAC (Supplementary Fig. 9), globally a statistically significant trend of $-40\,\mathrm{mm\,year^{-1}}$ is found (Fig. 4). We have concluded that for a 1 °C warming of SST, the TC-related surface freshwater flux reduces by 86% compared to its 1980 value. On average, global mean SST has increased by ~0.02 °C year^{-1} since 1980 (Supplementary Fig. 10a) and is inversely correlated with the TC-related surface freshwater flux ($r = -0.65$). Similarly, average TC size increases by 6 km with 1 °C of SST warming and exhibits a statistically significant growth in the last four decades of 0.84 km year^{-1} (Supplementary Fig. 10b). Previously, Pérez-Alarcón et al.[17] found a positive correlation between TC size and moisture uptake for TC precipitation. In line with this, the TC-related surface freshwater flux decreases with increasing TC outer radius by 8 mm year^{-1} ($p < 0.1$), indicating an overall increase in TC-related precipitation. Similarly, previous studies[15–17] pointed out that strong TCs tend to gain more moisture for generating the associated precipitation than weak TCs. In fact, a stronger TC usually produces a higher rain rate[54]. Additionally, although we found a non-statistically significant relationship between TC-related surface freshwater flux and the accumulated cyclone energy (ACE) during the study period, it was statistically significant ($1.18\,\mathrm{mm\,day^{-1}\,10^{-4}\,kt^{-2}}$, $p < 0.05$) after 1990, when global ACE significantly decreased (Supplementary Fig. 10d), supporting the global reduction in the TC-related surface freshwater flux. Overall, the annual average of the Oceanic Niño Index and the interannual variability of SST, frequency, size and lifetime accumulated TC-induced evaporation and precipitation explain ~80.5% of the annual variability of TC-related surface freshwater flux.

DISCUSSION

This study investigated and quantified anomalous moisture fluxes during TCs globally and, therefore, their impacts on the global hydrological cycle. By applying a Lagrangian moisture tracking method[43,44] to many atmospheric parcel trajectories from the outputs of the Lagrangian FLEXPART model[39], we computed the anomalies in the surface freshwater flux during the TCs from 1980 to 2018 and the grid-to-grid trend in the surface freshwater flux budget. Although the Lagrangian

approach neglects liquid water and ice content in the atmosphere, the mixing of air parcels, and the evaporation of precipitating hydrometeors[43,44], this work represents the current state-of-the-art on the impacts of TCs on the global hydrological cycle.

The regions with positive anomalous surface freshwater fluxes induced by TC (Fig. 1) mostly agreed with the main moisture sources for the precipitation associated with them for each major ocean basin[15–17]. It is worth noting that Pérez-Alarcón et al.[15–17] identified some regions (e.g. Philippine Sea, South China Sea and eastern tropical Pacific Ocean) as moisture sources for the precipitation within the TCs outer radius that we identified here as sink regions. That means the evaporation from these regions contributes to the precipitation produced by TCs; however, in terms of the water budget, the TC-induced evaporation in these areas is lesser than the induced precipitation. Overall, TCs induced higher evaporation than the climatological value for analogous dates of TC occurrence and similarly induced precipitation above climatological values over the sink regions (negative surface freshwater flux). Despite the role of TCs in the annual rainfall amounts over Southern Asia[6], we detected a statistically significant ($p < 0.05$) decrease in the absolute value of the negative surface freshwater flux in these regions during TCs on the same dates over the study period. This contradictory result underlines the fact that most TCs occur during the summer and autumn monsoon seasons, two periods with particularly high values of moisture transport from the ocean (and associated precipitation over land), independent of TCs occurrence. Previously, Chen et al.[55] noted that TC activity and seasonal monsoon climate may contribute in opposite manners to total rainfall in southern Asia, leading to complex interannual variability. Most recently, Chen et al.[56] detected that the early onset of the South China Sea summer monsoon after the 1990s favoured positive heating anomalies over South China, strengthening the East Asia Summer Monsoon and monsoon-related precipitation.

The spatial distribution of TC-related surface freshwater flux (Fig. 1 and Supplementary Fig. 2) reveals that TC frequency controls the impact of TCs on the global hydrological cycle. Large-scale and regional thermodynamic and dynamic conditions govern TC activity [e.g. ref. [57]] and thus influence TC-related moisture transport patterns. The highest impact of TCs on the global water budget detected during the peak Northern Hemisphere TC activity in August and September (Supplementary Fig. 2) is probably closely related to the highest SSTs, which play a critical role in regulating global atmospheric circulation[58], and the maximum northward equatorial position of tropical rain belts[59]. Although Sobel et al.[60] emphasised that global heat or moisture budgets are not useful for explaining the global number of TCs, seasonal TC frequency largely controls TC-related contributions to the global hydrological cycle.

The overall influence of ENSO on the annual TC-related surface freshwater flux, as shown in Fig. 2, is linked to the impact of ENSO on TC frequency in each basin. In the Pacific Ocean, TC activity was enhanced during El Niño years[61,62], whereas the NATL and Australian regions exhibited an overall reduction in the number of TCs[60,62]. The increase in anomalous moisture transport in the Pacific Ocean during El Niño events can also be attributed to convective anomalies over the western and central equatorial Pacific[63]. Conversely, the reduction in surface freshwater flux in the NATL basin is a response to the decrease in TC activity due to eastward displaced deep convection in the tropical Pacific, which enhances wind shear in the Atlantic Ocean[62], the reduction in moist convection[64] and the weakening of northeasterly trade in the tropical Atlantic Ocean[65]. Nonetheless, the warm phase of ENSO intensifies the Caribbean Low-Level jet[66,67], explaining the intensification of the TC-related surface freshwater flux over the Caribbean Sea in the NATL basin (Fig. 2). El Niño also enhances the negative surface freshwater flux over South Asia owing to the abnormal integrated vapour transport associated with westerly winds from the Indian Ocean and northern to southern China[68]. It also correlates negatively with TC-induced precipitation in the southern US[69], which explains the reduction in anomalous moisture flux in this region. The surface freshwater flux differences in the Indian Ocean between the warm and cold phases of ENSO were noticeably weaker than those in the remaining basins. El Niño slightly increased the moisture supply from the Arabian Sea and southern Bay of Bengal (Fig. 2); however, this response was not significant in terms of changes in TC frequency[62]. TCs activity over the SIO was also substantially influenced by ENSO, which enhanced (suppressed) the number of TCs west of 75°E during El Niño (La Niña) years and exhibited an opposite tendency east of 75°E[60,62]. The surface freshwater flux differences in the SIO exhibited eastward intensification and westward weakening (Fig. 2c, d), in line with the moisture source and transport patterns associated with TCs in that region[16]. Overall, the changes in large-scale mechanisms induced by ENSO influence the TC-related surface freshwater flux patterns in each basin by controlling the annual TC count. Nonetheless, more in-depth regional studies are needed to further investigate the modulatory role of ENSO in the anomalous surface freshwater flux in each basin.

Meanwhile, the overall statistically significant decreasing trend in the TC-related surface freshwater flux (Fig. 3) indicates that TC-induced precipitation has increased over the source areas or evaporation has increased over the sink regions, as revealed in Supplementary Fig. 9. Chauvin et al.[26] pointed out that moisture support from evaporation decreases with increasing TC-rainfall intensities; however, this behaviour is not captured when evaluating the lifetime accumulated TC-induced evaporation and precipitation (Supplementary Fig. 7). Additionally, our results suggest that the reduction in the TC-related surface freshwater flux also results from a slight decrease in TC frequency (Supplementary Fig. 4) and lifetime (Supplementary Fig. 8) in the last two decades and to a significant rise in SST (Supplementary Fig. 10a) over the study period. If this relationship remains invariable, we can hypothesise that in a warmer climate the global TC-induced precipitation will be higher than the TC-induced evaporation. Therefore, the increasing low-level moisture availability at a rate of 6–7% per degree of SST rising using the Clausius–Clapeyron relationship[32–34] in response to increasing evaporation due to global warming[70] can compensate for the reduction in TC-induced evaporation in regions far from the TC circulation and support the additional moisture required for excess TC-induced precipitation. Previous studies [e.g. ref. [71]] have detected tropical precipitation change rates higher than that predicted from the Clausius–Clapeyron relationship. They argued that these super Clausius–Clapeyron rates of changes (rates of change larger than those predicted according to the Clausius–Clapeyron relationship) are linked to enhanced TC dynamics, which will compensate for latent heat release from TC precipitation, favouring rainfall intensity itself. As previously noted, surface evaporation from the TC underlying surface is lesser than TC-induced precipitation within the outer radius (Supplementary Fig. 9), confirming the role of the moisture flux convergence in supporting moisture for TCs from external sources[26,27,72]. The contribution of moisture flux convergence in the water budget is additive and should lead to supper Clausius–Clapeyron rates of changes[25,26,73]. This previous relationship supports the rate of changes of the TC-induced surface freshwater flux with increasing SST, which projects that in a warming world the TC-induced precipitation, including those that occurred outer of TC circulation during moisture transport towards TC locations, will be higher than the total TC-induced evaporation. Therefore, the water vapour deficit should be supplied by the increasing low-level moisture availability

with SST rising. However, care must be taken in interpreting the decreasing TC-related surface freshwater flux with rising SST, firstly because the rate of changes were computed based on the annual value in 1980, and second, because the role of TCs in future changes in the hydrological cycle is not entirely clear within the scope of an inevitably warming world. We also acknowledge that a comprehensive assessment of the relationship between TCs and SSTs is rather more complex, as it must include other components not considered in our analysis. TC-related surface freshwater flux can modify the upper-ocean responses through its effects on sea surface salinity, causing sea surface freshening and enhancing stratification, which reduces oceanic mixing and SST cooling, resulting in a positive feedback to TC intensification [e.g. refs. [74,75]]. Meanwhile, TC-induced surface wind stress has the opposite effect, leading to SST cooling, resulting in a negative feedback on the TC intensity through its impact on air-sea enthalpy fluxes [e.g. refs. [76–80]]. Overall, the feedback from TCs to SST is controlled by a balance between the momentum flux of the storm and turbulent mixing in the upper ocean, and their relative magnitudes [e.g. ref. [75]]. This relationship should be further investigated under global warming to understand the full impact of TCs on the global water cycle under climate change.

Additionally, based on the robustness of future reductions in the global frequency of TCs in response to global warming[81,82], a reduction in surface freshwater flux induced by TCs is expected in the future. However, the results of Pérez-Alarcón et al.[15–17] revealed that intense TCs tend to gain more moisture to produce precipitation and therefore induce stronger moisture transport than weak TCs. Additionally, several studies [e.g. refs. [81,83]] have indicated an increase in the number of intense TCs. Based on these previous findings, moisture transport related to the growth of intense TCs under global warming can compensate for the reduction in surface freshwater flux caused by the projected decrease in global TC count. Given the profound impact of global warming on TC frequency and intensity[81,82,84], low-level moisture availability, column-integrated moisture[32–34], TC-related rainfall[85] and atmospheric circulation patterns[86], it is necessary to investigate the role of TC in hydrological cycles under climate change. This topic will be addressed in future studies.

In summary, the role of TCs in the hydrological cycle is strongly modulated by seasonal TC activity. This study confirms that TCs globally induce more evaporation and precipitation from moisture source and sink regions, respectively. Nonetheless, we provided evidence of a statistically significant globally decrease in TC-related surface freshwater flux, which could be attributed to a slight reduction of global TC frequency and lifetime in the last two decades. Additionally, we detected that TC-induced surface freshwater flux decreases approximately 86% per °C of SST warming. However, it should be noted that this rate of changes was estimated by comparing with TC-related surface freshwater flux in 1980. Overall, this study quantified the impact of TCs on global water budgets.

METHODS

TC data

The observed TC trajectories for the North Atlantic and NE Pacific were obtained from the HURDAT2 dataset[87] provided by the US National Hurricane Center. The US Joint Typhoon Warning Center provided information on TCs in the remaining basins. These datasets contain the records at 6-h intervals (synoptic times), although HURDAT2 includes entries at non-synoptic times to indicate intensity maxima or landfalling. There have been approximately 100 years of TC records in some basins [e.g. ref. [87]]; however, historical TC data have had the highest quality for climatological analysis since the beginning of satellite observations in the 1980s[88]. The TCSize dataset[89] provided the outer radii of all the TCs within the study period.

FLEXPART model simulations

The FLEXible PARTicle dispersion model (FLEXPART) model[39] is a Lagrangian model for tracking atmospheric moisture along air parcel trajectories. It was fed by the 6-h European Centre for Medium-Range Weather Forecast ERA-Interim reanalysis[45] with 61 vertical levels and $1° \times 1°$ grid spacing in latitude and longitude. ERA-Interim data were available from 1979 to August 2019. Therefore, the study period was from 1980 to 2018.

Despite the coarse grid spacing of ERA-Interim data, the FLEXPART model forced with this reanalysis has been widely used to investigate the source-sinks relationship associated with different weather systems, i.e., atmospheric rivers[90], extratropical[91], subtropical[92], and tropical cyclones[15–17,27]. Likewise, Fernández-Alvarez et al.[93] recently detected no significant differences between source-sink patterns from FLEXPART outputs forced with ERA-Interim and ERA5 reanalysis. Additionally, we acknowledge that several authors [e.g. refs. [26,94]] have addressed the inability of ERA-Interim to capture extreme precipitation associated with TCs. Nonetheless, Pérez-Alarcón et al.[27] highlighted that TC-related precipitation estimated from the Lagrangian approach, using ERA-Interim as input data for the FLEXPART model, fits well with observations.

On this basis, the model version and simulation design were the same as those used by Pérez-Alarcón et al.[15–17] to identify the moisture sources for precipitation produced by TCs during their three well-known stages of development (genesis, lifetime maximum intensity, and dissipation). FLEXPART requires three-dimensional (temperature and specific humidity, horizontal and vertical wind components) and two-dimensional (total cloud cover, 10 m horizontal wind components, surface pressure, large-scale and convective precipitation, east/west and north/south surface stress, 2 m temperature and dew point temperature, topography, land-sea mask and subgrid standard deviation of topography, and sensible heat flux) fields as input data. To account for subgrid convective transport and turbulence in the planetary boundary layer, FLEXPART uses the convection parameterisation scheme proposed by Emanuel and Živković-Rothman[95] and solves the Langevin equations for Gaussian turbulence[96], respectively.

During the simulations, FLEXPART divided the atmosphere into approximately two million air parcels of equal mass that were uniformly distributed, and the three-dimensional wind field advected air parcels throughout the atmosphere. We obtained the model outputs at a 6-h time step containing the information of each parcel, that is, position in latitude, longitude, and specific humidity.

Quantification of the anomalous moisture uptake

To estimate the water budget linked to the TCs, we backtracked the air parcels residing within the area delimited by the outer radius of the TCs at each system location for up to 10 days (240 h), which is considered the average time spent by moisture in the atmosphere from evaporation to precipitation[97]. Along the parcel pathways, the changes in specific humidity (q, expressed in g kg^{-1}) with time ($dt = 6$ h) respond to moisture increases and decreases by evaporation (e) and precipitation (p), respectively, as illustrated by the Lagrangian water budget equation[43,44] (Eq. 1).

$$(e - p) = m\frac{dq}{dt} \quad (1)$$

where m is the parcel mass (expressed in kg) and the left term (e-p) represents the freshwater flux of the parcel. By solving Eq. (1) for all parcels and amassing (e-p) over all N parcels residing in the atmospheric column over an area A ($1° \times 1°$), we estimated the

surface freshwater flux (*E-P*) as follows:

$$(E-P) \approx \frac{\sum(e-p)}{A} \quad (2)$$

Backward analysis revealed the origin of the moisture in air masses during TCs events. That is, TCs induce net evaporation when ($E\text{-}P > 0$) and net precipitation when ($E\text{-}P < 0$). Therefore, regions in which evaporation (precipitation) exceeds precipitation (evaporation) can be considered moisture sources (sinks).

For each TC position, the climatological surface freshwater flux (including TC's surface freshwater flux) was computed by averaging the surface freshwater flux for the same location and time step (month, day, and hour) of the TC over the study period. Thus, we verified whether the predominant evaporation (precipitation) areas during the TCs differed from the climatology by estimating surface freshwater flux anomalies. The surface freshwater flux anomalies for the TC time were obtained as the difference between the surface freshwater flux associated with the TC and the climatological flux.

TC-induced precipitation and evaporation within the outer radius

To account for the lifetime accumulated TC-induced precipitation (evaporation), we summed over the TC lifetime the total precipitation (evaporation) within a circle centred on the moving TC. All precipitation (evaporation) events within the TC outer radius are attributable to TCs. Previously, Lavender and McBride[53] and Hallam et al.[52] applied a similar approach to compute TC-related precipitation totals. TC-induced precipitation was extracted from the Multi-Source Weighted-Ensemble Precipitation V2 (MSWEP) database[51]. The MSWEP has high spatial ($0.1° \times 0.1°$ grid spacing) and temporal (3 h) resolutions and covers a long period (1979–present). It integrates observations from different data sources, e.g. surface rainfall gauge stations, satellite and reanalysis data. Additionally, it uses global streamflow observations at 13,762 stations for bias correction. Meanwhile, we computed TC-induced evaporation from the ERA-Interim reanalysis.

Annual mean sea surface temperature

As we are interested in the sea surface temperature (SST) during the TC occurrence, we used the US National Oceanic and Atmospheric Administration Daily Optimum Interpolation Sea Surface Temperature (OISST) dataset[50] to compute the annual mean SST at basin and global scale. This dataset merges observations from different platforms, such as satellites, ships and buoys, into a regular global grid of $0.25° \times 0.25°$ in latitude and longitude. This dataset is available from September 1981 to the present. Thus, the analysis that included SST data was performed from 1982 to 2018. For each basin, we average the SST within the limited area by the highest TC activity (Supplementary Fig. 5) during TC occurrence, while for the global mean SST we average the SST of all the basins during TC dates.

Classification of ENSO years

To classify a TC season under El Niño La Niña, we followed the procedure of the US Climate Prediction Center based on the Ocean Niño Index (ONI, 3-month running mean of sea surface temperature anomalies in Niño 3.4 region). A year was classified as El Niño (La Niña) if the ONI remained higher (lower) than 0.5°C (−0.5 °C) for at least 5 consecutive months. If neither of these conditions was satisfied, the year was classified as an ENSO-neutral year. This approach was previously applied by Pérez-Alarcón et al.[97] and Colbert and Soden[98] to investigate the impact of the ENSO on the trajectories and moisture sources of the North Atlantic TCs formed in the main development region.

DATA AVAILABILITY

The HURDAT2 database provided by the National Hurricane Center and the best track archives from the Joint Warning Typhoon Center are freely available at https://www.nhc.noaa.gov/data/#hurdat and https://www.metoc.navy.mil/jtwc/jtwc.html?best-tracks, respectively. The TCSize dataset can be freely downloaded from https://doi.org/10.17632/8997r89fbf.1. The ERA-Interim reanalysis supported by the European Centre for Medium-Range Weather Forecasts can be retrieved from https://apps.ecmwf.int/datasets/data/interim-full-daily/levtype=sfc/. MSWEP is available at http://www.gloh2o.org/mswep/ and the OISST database can be obtained from https://www.ncei.noaa.gov/products/optimum-interpolation-sst. The Ocean Niño Index (ONI) was obtained from the US National Oceanic and Atmospheric Administration - Physical Sciences Laboratory at https://psl.noaa.gov/data/climateindices/list/. The Lagrangian moisture tracking method described in the 'Methods' section have been coded in Python in the TRansport Of water Vapor (TROVA) tool[99], which is freely available at https://github.com/ElsevierSoftwareX/SOFTX-D-22-00100. Meanwhile, the FLEXPART source code is available at https://www.flexpart.eu/downloads/6.

Received: 21 July 2023; Accepted: 6 December 2023;
Published online: 18 December 2023

REFERENCES

1. Emanuel, K. Contribution of tropical cyclones to meridional heat transport by the oceans. *J. Geophys. Res.* **106**, 14771–14781 (2001).
2. Mohamed, H. A. B., Husin, M. A. & Hasanen, H. M. Kinetic energy budget of a tropical cyclone. *Atmos. Clim. Sci.* **5**, 394 (2015).
3. Xu, G., Osborn, T. J. & Matthews, A. J. Moisture transport by Atlantic tropical cyclones onto the North American continent. *Clim. Dyn.* **48**, 3161–3182 (2017).
4. Guo, L. et al. Contribution of tropical cyclones to atmospheric moisture transport and rainfall over East Asia. *J. Clim.* **30**, 3853–3865 (2017).
5. Peduzzi, P. et al. Global trends in tropical cyclone risk. *Nat. Clim. Chang.* **2**, 289–294 (2012).
6. Khouakhi, A., Villarini, G. & Vecchi, G. A. Contribution of tropical cyclones to rainfall at the global scale. *J. Clim.* **30**, 359–372 (2017).
7. Yang, X., Zhou, L., Zhao, C. & Yang, J. Impact of aerosols on tropical cycloneinduced precipitation over the mainland of China. *Clim. Chang.* **148**, 173–185 (2018).
8. Gimeno, L., Nieto, R., Vázquez, M. & Lavers, D. A. Atmospheric rivers: a mini-review. *Front. Earth Sci.* **2**, 2 (2014).
9. Brun, J. & Barros, A. P. Mapping the role of tropical cyclones on the hydroclimate of the southeast United States: 2002–2011. *Int. J. Climatol.* **34**, 494–517 (2014).
10. Zhao, C. et al. Enlarging rainfall area of tropical cyclones by atmospheric aerosols. *Geophys. Res. Lett.* **45**, 8604–8611 (2018).
11. Bieli, M., Camargo, S. J., Sobel, A. H., Evans, J. L. & Hall, T. A global climatology of extratropical transition. Part I: Characteristics across basins. *J. Clim.* **32**, 3557–3582 (2019).
12. Gray, W. M. A global view of the origin of tropical disturbances and storms. *Mon. Weather Rev.* **96**, 669–700 (1968).
13. Emanuel, K., DesAutels, C., Holloway, C. & Korty, R. Environmental control of tropical cyclone intensity. *J. Atmos. Sci.* **61**, 843–858 (2004).
14. Ge, X., Li, T. & Peng, M. Effects of vertical shears and midlevel dry air on tropical cyclone developments. *J. Atmos. Sci.* **70**, 3859–3875 (2013).
15. Pérez-Alarcón, A., Sorí, R., Fernández-Alvarez, J. C., Nieto, R. & Gimeno, L. Where does the moisture for North Atlantic tropical cyclones come from? *J. Hydrometeorol.* **23**, 457–472 (2022).
16. Pérez-Alarcón, A., Fernández-Alvarez, J. C., Sorí, R., Nieto, R. & Gimeno, L. Moisture source identification for precipitation associated with tropical cyclone development over the Indian Ocean: a Lagrangian approach. *Clim. Dyn.* **60**, 2735–2758 (2023).
17. Pérez-Alarcón, A., Sorí, R., Fernández-Alvarez, J. C., Nieto, R. & Gimeno, R. Moisture source for the precipitation of tropical cyclones over the Pacific Ocean through a Lagrangian approach. *J. Clim.* **36**, 1059–1083 (2023).
18. Chu, Q. C., Wang, Q. G. & Feng, G. L. Determination of the major moisture sources of cumulative effect of torrential rain events during the preflood season over South China using a Lagrangian particle model. *J. Geophys. Res. Atmos.* **122**, 8369–8382 (2017).
19. Vázquez, M., Nieto, R., Liberato, M. L. R. & Gimeno, L. Atmospheric moisture sources associated with extreme precipitation during the peak precipitation month. *Weather Clim. Extremes* **30**, 100289 (2020).
20. Trenberth, K. E., Dai, A., Rasmussen, R. M. & Parsons, D. B. The changing character of precipitation. *Bull. Am. Meteorol. Soc.* **84**, 1205–1217 (2003).

21. Braun, S. A. High-resolution simulation of Hurricane Bonnie (1998). Part II: Water budget. *J. Atmos. Sci.* **63**, 43–64 (2006).
22. Trenberth, K. E. & Fasullo, J. Water and energy budgets of hurricanes and implications for climate change. *Geophys. Res. Atmos.* **112**, D23107 (2007).
23. Yang, M. J., Braun, S. A. & Chen, D. S. Water budget of typhoon Nari (2001). *Mon. Weather Rev.* **139**, 3809–3828 (2011).
24. Wu, W., Chen, J. & Huang, R. Water budgets of tropical cyclones: three case studies. *Adv. Atmos. Sci.* **30**, 468–484 (2013).
25. Wang, C. C., Lin, B. X., Chen, C. T. & Lo, S. H. Quantifying the effects of long-term climate change on tropical cyclone rainfall using a cloud-resolving model: examples of two landfall typhoons in Taiwan. *J. Clim.* **28**, 66–85 (2015).
26. Chauvin, F., Douville, H. & Ribes, A. Atlantic tropical cyclones water budget in observations and CNRM-CM5 model. *Clim. Dyn.* **49**, 4009–4021 (2017).
27. Pérez-Alarcón, A. et al. Moisture sources for precipitation associated with major hurricanes during 2017 in the North Atlantic basin. *J. Geophys. Res. Atmos.* **127**, e2021JD035554 (2022).
28. Dominguez, C. & Magaña, V. The role of tropical cyclones in precipitation over the tropical and subtropical North America. *Front. Earth Sci.* **6**, 19 (2018).
29. Liu, Q., Li, T. & Zhou, W. Impacts of multi-timescale circulations on meridional moisture transport. *J. Clim.* **34**, 8065–8085 (2021).
30. Liu, M., Smith, J. A., Yang, J. A. & Vecchi, G. A. Tropical cyclone flooding in the Carolinas. *J. Hydrometeorol.* **23**, 53–70 (2022).
31. Collier, E., Sauter, T., Mölg, T. & Hardy, D. The influence of tropical cyclones on circulation, moisture transport, and snow accumulation at Kilimanjaro during the 2006–2007 season. *J. Geophys. Res. Atmos.* **124**, 6919–6928 (2019).
32. O'Gorman, P. & Muller, C. J. How closely do changes in surface and column water vapor follow Clausius–Clapeyron scaling in climate change simulations? *Environ. Res. Lett.* **5**, 025207 (2010).
33. Allan, R. P. The role of water vapour in Earth's energy flows. *Surv. Geophys* **33**, 557–564 (2012).
34. Bao, J., Sherwood, S. C., Alexander, L. V. & Evans, J. P. Future increases in extreme precipitation exceed observed scaling rates. *Nat. Clim. Chang.* **7**, 128–132 (2017).
35. Gimeno, L. et al. Oceanic and terrestrial sources of continental precipitation. *Rev. Geophys.* **50**, RG4003 (2012).
36. Gimeno, L. et al. Recent progress on the sources of continental precipitation as revealed by moisture transport analysis. *Earth Sci. Rev.* **201**, 103070 (2020).
37. Cheng, T. F. & Lu, M. Global Lagrangian tracking of continental precipitation recycling, footprints, and cascades. *J. Clim.* **36**, 1923–1941 (2023).
38. Staal, A., Koren, G., Tejada, G. & Gatti, L. V. Moisture origins of the Amazon carbon source region. *Environ. Res. Lett.* **18**, 044027 (2023).
39. Stohl, A., Forster, C., Frank, A., Seibert, P. & Wotawa, G. The Lagrangian particle dispersion model FLEXPART version 6.2. *Atmos. Chem. Phys.* **5**, 2461–2474 (2005).
40. Kunkel, K. E. & Champion, S. M. An assessment of rainfall from Hurricanes Harvey and Florence relative to other extremely wet storms in the United States. *Geophys. Res. Lett.* **46**, 13500–13506 (2019).
41. Gao, S., Mao, J., Zhang, W., Zhang, F. & Shen, X. Atmospheric moisture shapes increasing tropical cyclone precipitation in southern China over the past four decades. *Environ. Res. Lett.* **16**, 034004 (2021).
42. Kim, D., Park, D. S. R., Nam, C. C. & Bell, M. M. The parametric hurricane rainfall model with moisture and its application to climate change projections. *npj Clim. Atmos. Sci.* **5**, 86 (2022).
43. Stohl, A. & James, P. A. Lagrangian analysis of the atmospheric branch of the global water cycle. Part I: method description, validation, and demonstration for the August 2002 flooding in central Europe. *J. Hydrometeorol.* **5**, 656–678 (2004).
44. Stohl, A. & James, P. A. Lagrangian analysis of the atmospheric branch of the global water cycle. Part II: Moisture transports between earth's ocean basins and river catchments. *J. Hydrometeorol.* **6**, 961–984 (2005).
45. Dee, D. P. et al. The ERA-Interim reanalysis: configuration and performance of the data assimilation system. *QJR Meteorol. Soc.* **137**, 553–597 (2011).
46. Xian, P. & Miller, R. L. Abrupt seasonal migration of the ITCZ into the summer hemisphere. *J. Atmos. Sci.* **65**, 1878–1895 (2008).
47. Nieto, R., Ciric, D., Vázquez, M., Liberato, M. L. & Gimeno, L. Contribution of the main moisture sources to precipitation during extreme peak precipitation months. *Adv. Water Resour.* **131**, 103385 (2019).
48. Gao, S., Zhu, L., Zhang, W. & Shen, X. Western North Pacific tropical cyclone activity in 2018: a season of extremes. *Sci. Rep.* **10**, 5610 (2020).
49. Zhao, H. & Raga, G. B. On the distinct interannual variability of tropical cyclone activity over the eastern North Pacific. *Atmósfera* **28**, 161–178 (2015).
50. Huang, B. et al. Improvements of the daily optimum interpolation sea surface temperature (DOISST) version 2.1. *J. Clim.* **34**, 2923–2939 (2021).
51. Beck, H. E. et al. MSWEP V2 global 3-hourly 0.1 precipitation: methodology and quantitative assessment. *Bull. Am. Meteorol. Soc.* **100**, 473–500 (2019).
52. Hallam, S. et al. The relationship between sea surface temperature anomalies, wind and translation speed and North Atlantic tropical cyclone rainfall over ocean and land. *Environ. Res. Commun.* **5**, 025007 (2023).
53. Lavender, S. L. & McBride, J. L. Global climatology of rainfall rates and lifetime accumulated rainfall in tropical cyclones: influence of cyclone basin, cyclone intensity and cyclone size. *Int. J. Climatol.* **41**, E1217–E1235 (2021).
54. Tu, S. et al. Recent global decrease in the inner-core rain rate of tropical cyclones. *Nat. Commun.* **12**, 1948 (2021).
55. Chen, J. M., Li,, T. & Shih, C. F. Tropical cyclone–and monsoon-induced rainfall variability in Taiwan. *J. Clim.* **23**, 4107–4120 (2010).
56. Chen, J. P., Wen, S. P. & Wang, X. Relationship over southern China between the summer rainfall induced by tropical cyclones and that by monsoon. *Atmos. Ocean Sci. Lett.* **10**, 96–103 (2017).
57. Murakami, H. & Wang, B. Patterns and frequency of projected future tropical cyclone genesis are governed by dynamic effects. *Commun. Earth Environ.* **3**, 77 (2022).
58. Song, J., Klotzbach, P. & Duan, Y. Differences in western North Pacific tropical cyclone activity among three El Niño phases. *J. Clim.* **33**, 7983–8002 (2020).
59. Biasutti, M. et al. Global energetics and local physics as drivers of past, present and future monsoons. *Nat. Geosci.* **11**, 392–400 (2018).
60. Sobel, A. H. et al. Tropical cyclone frequency. *Earth's Future* **9**, e2021EF002275 (2021).
61. Li, R. C. & Zhou, W. Changes in western Pacific tropical cyclones associated with the El Niño–Southern Oscillation cycle. *J. Clim.* **25**, 5864–5878 (2012).
62. Lin, I.-I., et al. in *El Niño Southern Oscillation in a Changing Climate* (eds McPhaden, M. J., Santoso, A. & Cai, W.) Ch. 17 (American Geophysical Union, 2020).
63. Taschetto, A. S., Rodrigues, R. R., Meehl, G. A., McGregor, S. & England, M. H. How sensitive are the Pacific–tropical North Atlantic teleconnections to the position and intensity of El Niño-related warming? *Clim. Dyn.* **46**, 1841–1860 (2016).
64. Jiang, L. & Li, T. Relative roles of El Niño-induced extratropical and tropical forcing in generating Tropical North Atlantic (TNA) SST anomaly. *Clim. Dyn.* **53**, 3791–3804 (2019).
65. García-Serrano, J., Cassou, C., Douville, H., Giannini, A. & Doblas-Feyes, F. J. Revisiting the ENSO teleconnection to the tropical North Atlantic. *J. Clim.* **30**, 6945–6957 (2017).
66. Durán-Quesada, A. M., Gimeno, L. & Amador, J. Role of moisture transport for Central American precipitation. *Earth Syst. Dyn.* **8**, 147–161 (2017).
67. Amador, J. A. The Intra-Americas sea low-level jet. *Ann. NY Acad. Sci.* **1146**, 153–188 (2008).
68. Wang, L., Yang, Z., Gu, X. & Li, J. Linkages between tropical cyclones and extreme precipitation over China and the role of ENSO. *Int. J. Disaster Risk Sci.* **11**, 538–553 (2020).
69. Nogueira, R. C., Keim, B. D., Brown, D. P. & Robbins, K. D. Variability of rainfall from tropical cyclones in the eastern USA and its association to the AMO and ENSO. *Theor. Appl. Climatol.* **112**, 273–283 (2013).
70. Gimeno, L., Vázquez, M., Nieto, R. & Trigo, R. M. Atmospheric moisture transport: the bridge between ocean evaporation and Arctic ice melting. *Earth Syst. Dyn.* **6**, 583–589 (2015).
71. Sugiyama, M., Shiogama, H. & Emori, S. Precipitation extreme changes exceeding moisture content increases in MIROC and IPCC climate models. *Proc. Natl Acad. Sci. USA* **107**, 571–575 (2010).
72. Makarieva, A. M. et al. Fuel for cyclones: the water vapor budget of a hurricane as dependent on its movement. *Atmos. Res.* **193**, 216–230 (2017).
73. Knutson, T. R. et al. Tropical cyclones and climate change. *Nat. Geosci.* **3**, 157–163 (2010).
74. Balaguru, K., Foltz, G. R., Leung, L. R. & Hagos, S. M. Impact of rainfall on tropical cyclone-induced sea surface cooling. *Geophys. Res. Lett.* **49**, e2022GL098187 (2022).
75. Ye, S., Zhang, R. H. & Wang, H. The role played by tropical cyclones-induced freshwater flux forcing in the upper-ocean responses: a case for Typhoon Yutu (2018). *Ocean Model.* **184**, 102211 (2023).
76. Balaguru, K., Foltz, G. R., Leung, L. R. & Emanuel, K. A. Global warming-induced upper-ocean freshening and the intensification of super typhoons. *Nat. Commun.* **7**, 13670 (2016).
77. Lloyd, I. D. & Vecchi, G. A. Observational evidence for oceanic controls on hurricane intensity. *J. Clim.* **24**, 1138–1153 (2011).
78. Mainelli, M., DeMaria, M., Shay, L. K. & Goni, G. Application of oceanic heat content estimation to operational forecasting of recent Atlantic category 5 hurricanes. *Weather Forecast* **23**, 3–16 (2008).
79. Karnauskas, K. B., Zhang, L. & Emanuel, K. A. The feedback of cold wakes on tropical cyclones. *Geophys. Res. Lett.* **48**, e2020GL091676 (2021).
80. Ma, Z., Fei, J., Lin, Y. & Huang, X. Modulation of clouds and rainfall by tropical cyclone's cold wakes. *Geophys. Res. Lett.* **47**, e2020GL088873 (2020).

81. Knutson, T. et al. Tropical cyclones and climate change assessment: Part II: Projected response to anthropogenic warming. *Bull. Am. Meteorol. Soc.* **101**, E303–E322 (2020).
82. Chand, S. S. et al. Declining tropical cyclone frequency under global warming. *Nat. Clim. Chang.* **12**, 655–661 (2022).
83. Kossin, J. P., Knapp, K. R., Olander, T. L. & Velden, C. S. Global increase in major tropical cyclone exceedance probability over the past four decades. *Proc. Natl Acad. Sci. USA* **117**, 11975–11980 (2020).
84. Pérez-Alarcón, A., Fernández-Alvarez, J. C. & Coll-Hidalgo, P. Global increase of the intensity of tropical cyclones under global warming based on their maximum potential intensity and CMIP6 models. *Environ. Process.* **10**, 36 (2023).
85. Patricola, C. M. & Wehner, M. F. Anthropogenic influences on major tropical cyclone events. *Nature* **563**, 339–346 (2018).
86. Sharmila, S. & Walsh, K. J. F. Recent poleward shift of tropical cyclone formation linked to Hadley cell expansion. *Nat. Clim. Chang.* **8**, 730–736 (2018).
87. Landsea, C. W. & Franklin, J. L. Atlantic Hurricane database uncertainty and presentation of a new database format. *Mon. Weather Rev.* **141**, 3576–3592 (2013).
88. Vecchi, G. A. & Knutson, T. R. On estimates of historical North Atlantic tropical cyclone activity. *J. Clim.* **21**, 3580–3600 (2008).
89. Pérez-Alarcón, A., Sorí, R., Fernández-Alvarez, J. C., Nieto, R. & Gimeno, L. Dataset of outer tropical cyclone size from a radial wind profile. *Data Brief.* **40**, 107825 (2022).
90. Ramos, R. et al. Atmospheric rivers moisture sources from a Lagrangian perspective. *Earth. Syst. Dyn.* **7**, 371–384 (2016).
91. Coll-Hidalgo, P., Pérez-Alarcón, A. & Gimeno, L. Origin of moisture for the precipitation produced by the exceptional winter storm formed over the Gulf of Mexico in March 1993. *Atmosphere* **13**, 1154 (2022).
92. Gozzo, L. F., Da Rocha, R. P., Gimeno, L. & Drumond, A. Climatology and numerical case study of moisture sources associated with subtropical cyclogenesis over the southwestern Atlantic Ocean. *J. Geophys. Res. Atmos.* **122**, 5636–5653 (2017).
93. Fernández-Alvarez, J. C., Vázquez, M., Pérez-Alarcón, A., Nieto, R. & Gimeno, L. Comparison of moisture sources and sinks estimated with different versions of FLEXPART and FLEXPART-WRF models forced with ECMWF reanalysis data. *J. Hydrometeorol.* **24**, 221–239 (2023).
94. Maoyi, M. L., Abiodun, B. J., Prusa, J. M. & Veitch, J. J. Simulating the characteristics of tropical cyclones over the South West Indian Ocean using a stretched-grid global climate model. *Clim. Dyn.* **50**, 1581–1596 (2018).
95. Emanuel, K. & Živković-Rothman, M. Development and evaluation of a convection scheme for use in climate models. *J. Atmos. Sci.* **56**, 1766–1782 (1999).
96. Stohl, A. & Thomson, D. J. A density correction for Lagrangian particle dispersion models. *Bound. Layer Meteorol.* **90**, 155–167 (1999).
97. Pérez-Alarcón, A. et al. Climatological variations of moisture sources for precipitation of North Atlantic tropical cyclones linked to their tracks. *Atmos. Res.* **290**, 106778 (2023).
98. Colbert, A. J. & Soden, B. J. Climatological variations in North Atlantic tropical cyclone tracks. *J. Clim.* **25**, 657–673 (2012).
99. Fernández-Alvarez, J. C., Pérez-Alarcón, A., Nieto, R. & Gimeno, L. TROVA: TRansport Of water VApor. *SoftwareX* **20**, 101228 (2022).

ACKNOWLEDGEMENTS

A.P.-A. thanks the support from the Xunta de Galicia (Galician Regional Government, Consellería de Cultura, Educación e Universidade) under the Postdoctoral grant No. ED481B-2023/016. J.C.F.-A. and P.C.-H. acknowledge support from the Xunta de Galicia (Consellería de Cultura, Educación e Universidade) under PhD grants No. ED481A2020/193 and ED481A2022/128, respectively. R.M.T. was supported by the Portuguese Science Foundation (FCT) through the project AMOTHEC (DRI/India/0098/2020). EPhysLab members are supported by SETESTRELO project (grant no. PID2021-122314OB-I00) funded by the Ministerio de Ciencia, Innovación y Universidades, Spain (MCIN/10.13039/501100011033) and Xunta de Galicia (grant ED431C2021/44; Programa de Consolidación e Estructuración de Unidades de Investigación Competitivas (Grupos de Referencia Competitiva), Consellería de Cultura, Educación e Universidade), and by "ERDF A way of making Europe". This work has also been possible thanks to the computing resources and technical support provided by Centro de Supercomputación de Galicia (CESGA) and the Red Española de Supercomputación (RES).

AUTHOR CONTRIBUTIONS

Conceptualisation: A.P.-A., R.N., L.G. Methodology: A.P.-A., R.N., L.G. Investigation: A.P.-A., P.C.-H., J.C.F.-A., R.M.T., R.N., L.G. Software: A.P.-A., J.C.F.-A. Visualisation: A.P.-A., P.C.-H., J.C.F.-A. Supervision: R.M.T., R.N., L.G. Writing—original draft: A.P.-A. Writing—review and editing: A.P.-A., P.C.-H., J.C.F.-A., R.M.T., R.N., L.G.

COMPETING INTERESTS

The authors declare no competing interests.

ADDITIONAL INFORMATION

Supplementary information The online version contains supplementary material available at https://doi.org/10.1038/s41612-023-00546-5.

Correspondence and requests for materials should be addressed to Luis Gimeno.

Reprints and permission information is available at http://www.nature.com/reprints

Publisher's note Springer Nature remains neutral with regard to jurisdictional claims in published maps and institutional affiliations.